RESEARCH ARTICLE SUMMARY

NEUROSCIENCE

A gut-brain neural circuit for nutrient sensory transduction

Melanie Maya Kaelberer, Kelly L. Buchanan, Marguerita E. Klein, Bradley B. Barth, Marcia M. Montoya, Xiling Shen, Diego V. Bohórquez*

INTRODUCTION: In 1853, Sydney Whiting wrote in his classic *Memoirs of a Stomach*, "...and between myself and that individual Mr. Brain, there was established a double set of electrical wires, by which means I could, with the greatest ease and rapidity, tell him all the occurrences of the day as they arrived, and he also could impart to me his own feelings and impressions." Historically, it is known that the gut must communicate with the brain, but the underlying neural circuits and transmitters mediating gut-brain sensory transduction still remain unknown. In the gut, there is a single layer of epithelial cells separating the lumen from the underlying tissue. Dispersed within this layer reside electrically excitable cells termed enteroendocrine cells, which sense ingested nutrients and microbial metabolites. Like taste or olfactory receptor cells, enteroendocrine cells fire action potentials in the presence of stimuli. However, unlike other sensory epithelial cells, no synaptic link between enteroendocrine cells and a cranial nerve has been described. The cells are thought to act on nerves only indirectly through the slow endocrine action of hormones, like cholecystokinin. Despite its role in satiety, circulating concentrations of cholecystokinin peak only several minutes after food is ingested and often after the meal has ended. Such a discrepancy suggests that the brain perceives gut sensory cues through faster neuronal signaling. Using a mouse model, we sought to identify the underpinnings of this neural circuit that transduces a sense from gut to brain.

RATIONALE: Our understanding of brain neural circuits is being propelled forward by the emergence of molecular tools that have high topographical and temporal precision. We adapted them for use in the gut. Single-cell quantitative real-time polymerase chain reaction and single-cell Western blot enabled the assessment of synaptic proteins. A monosynaptic rabies virus revealed the neural circuit's synapse. The neural circuit was recapitulated in vitro by using nodose neurons cocultured with either minigut organoids or purified enteroendocrine cells. This system, coupled to optogenetics and whole-cell patch-clamp recording, served to determine the speed of transduction. Whole-nerve electrophysiology, along with optical excitation and silencing, helped to uncover the neurotransmission properties of the circuit in vivo. The underlying neurotransmitter was revealed by using receptor pharmacology and a fluorescent reporter called iGluSnFR.

RESULTS: Single-cell analyses showed that a subset of enteroendocrine cells contains presynaptic adhesion proteins, including some necessary for synaptic adhesion. Monosynaptic rabies tracing revealed that enteroendocrine cells synapse with vagal nodose neurons. This neuroepithelial circuit connects the intestinal lumen with the brainstem in one synapse. In coculture, this connection was sufficient to transduce a sugar stimulus from enteroendocrine cells to vagal neurons. Optogenetic activation of enteroendocrine cells elicited excitatory postsynaptic potentials in connected nodose neurons within milliseconds. In vivo recordings showed that enteroendocrine cells are indeed necessary and sufficient to transduce a sugar stimulus to the vagus. By using iGluSnFR, we found that enteroendocrine cells synthesize the neurotransmitter glutamate, and pharmacological inactivation of cholecystokinin and glutamate receptors revealed that these cells use glutamate as a neurotransmitter to transduce fast, sensory signals to vagal neurons.

ON OUR WEBSITE

Read the full article at http://dx.doi.org/10.1126/science.aat5236

CONCLUSION: We identified a type of gut sensory epithelial cell that synapses with vagal neurons. This cell has been referred to as the gut endocrine cell, but its ability to form a neuroepithelial circuit calls for a new name. We term this gut epithelial cell that forms synapses the neuropod cell. By synapsing with the vagus nerve, neuropod cells connect the gut lumen to the brainstem. Neuropod cells transduce sensory stimuli from sugars in milliseconds by using glutamate as a neurotransmitter. The neural circuit they form gives the gut the rapidity to tell the brain of all the occurrences of the day, so that he, too, can make sense of what we eat. ■

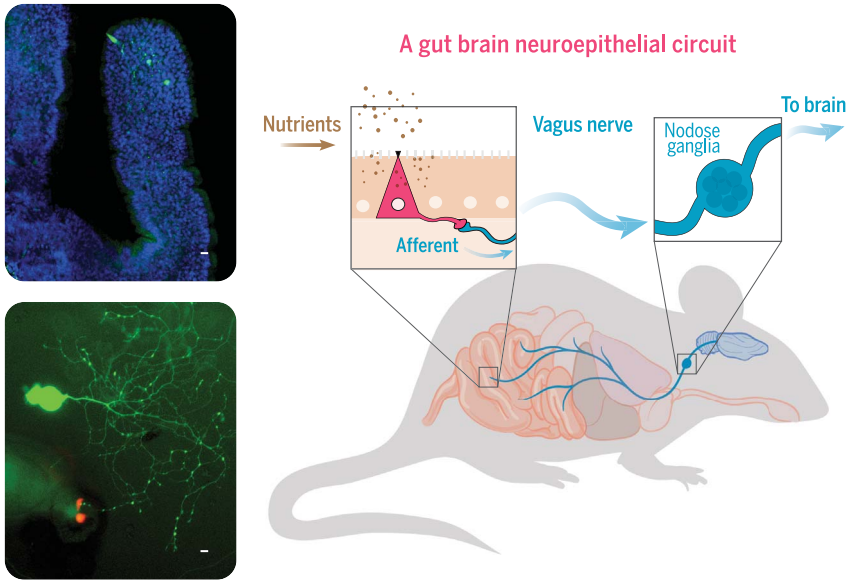

The neuropod cells. (Top left) Neuropod cells synapse with sensory neurons in the small intestine, as shown in a confocal microscopy image. Blue indicates all cells in villus; green indicates green fluorescent protein (GFP) in neuropod cell and sensory neurons. (Bottom left) This neural circuit is recapitulated in a coculture system between organoids and vagal neurons. Green indicates GFP in vagal neuron; red indicates tdTomato red fluorescence in neuropod cell. (Right) Neuropod cells transduce fast sensory signals from gut to brain. Scale bars, 10 μm.

The list of author affiliations is available in the full article online.
*Corresponding author. Email: diego.bohorquez@duke.edu
Cite this article as M. M. Kaelberer *et al.*, *Science* **361**, eaat5236 (2018). DOI: 10.1126/science.aat5236

RESEARCH ARTICLE

NEUROSCIENCE

A gut-brain neural circuit for nutrient sensory transduction

Melanie Maya Kaelberer[1], Kelly L. Buchanan[2], Marguerita E. Klein[1], Bradley B. Barth[3], Marcia M. Montoya[3], Xiling Shen[3], Diego V. Bohórquez[1,4,5]*

The brain is thought to sense gut stimuli only via the passive release of hormones. This is because no connection has been described between the vagus and the putative gut epithelial sensor cell—the enteroendocrine cell. However, these electrically excitable cells contain several features of epithelial transducers. Using a mouse model, we found that enteroendocrine cells synapse with vagal neurons to transduce gut luminal signals in milliseconds by using glutamate as a neurotransmitter. These synaptically connected enteroendocrine cells are referred to henceforth as neuropod cells. The neuroepithelial circuit they form connects the intestinal lumen to the brainstem in one synapse, opening a physical conduit for the brain to sense gut stimuli with the temporal precision and topographical resolution of a synapse.

Whereas touch, sight, sound, scent, and taste are transduced to the brain by innervated epithelial sensor cells (*1*), perception of gut stimuli is thought to occur only indirectly, through the slow action of hormones (*2*). The putative gut epithelial sensor cells—enteroendocrine cells—are assumed to lack synapses with the cranial nerve that innervates the viscera—the vagus (*3*).

Coined in the 1930s (*4*), the term enteroendocrine is rooted in the notion that nutrients stimulate the release of hormones. These neuropeptides either enter the bloodstream or act on nearby nerves minutes to hours after ingesting a meal (*5*). But enteroendocrine cells have several features of epithelial transducers: They have mechanical (*6*), olfactory (*7*), and taste (*8*) receptors; their membranes contain voltage-gated ion channels that render them electrically excitable (*9*); and they are capable of forming synapses (*10*). Almost two-thirds of enteroendocrine cells synapse with adjacent nerves in the intestinal and colonic mucosa (*10*). Similar features have been confirmed in a subset of colonic enteroendocrine cells known as enterochromaffin (*11*). Therefore, we hypothesized that enteroendocrine cells synapse with the vagus to transduce a sense from gut to brain.

Innervated epithelial sensors in the gut

Using mass spectroscopy (see methods and table S1), we confirmed that enteroendocrine cells express multiple neuropeptides (*12*, *13*), including both cholecystokinin (CCK) and peptide YY (PYY). Thus, we identified these cells using CCK and

[1]Department of Medicine, Duke University, Durham, NC, USA. [2]School of Medicine, Duke University, Durham, USA, NC. [3]Department of Biomedical Engineering, Duke University, Durham, NC, USA. [4]Department of Neurobiology, Duke University, Durham, NC, USA. [5]Duke Institute for Brain Sciences, Duke University, Durham, NC, USA.
*Corresponding author. Email: diego.bohorquez@duke.edu

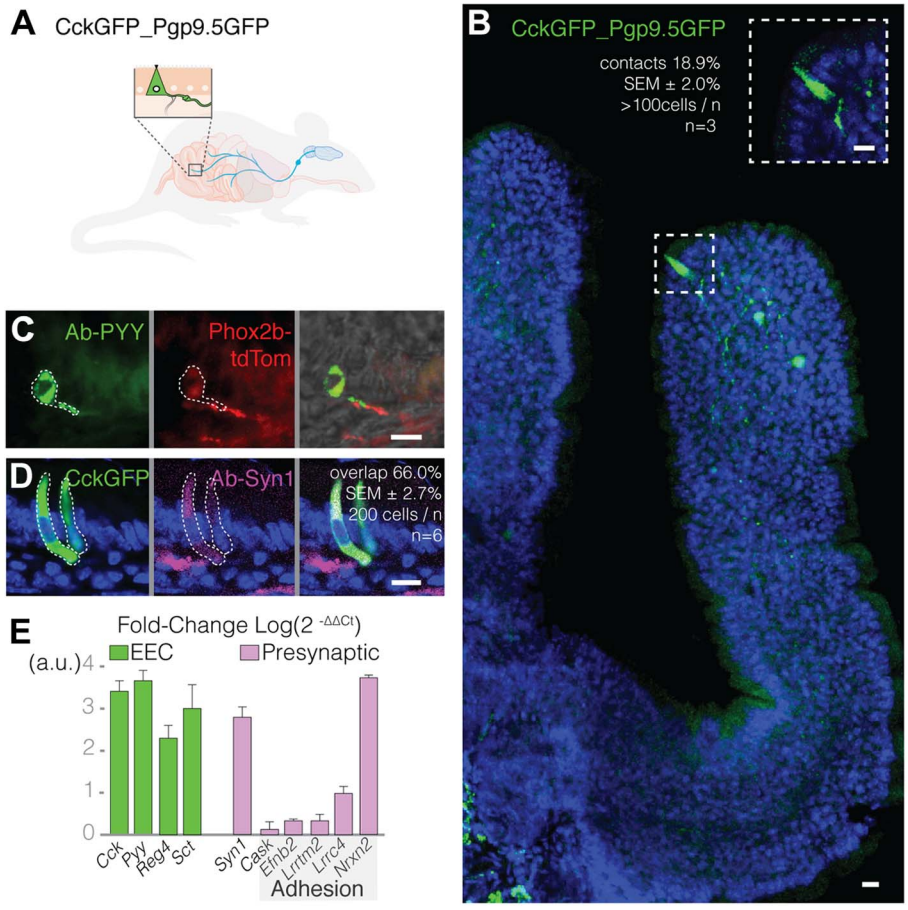

Fig. 1. Enteroendocrine cells contact sensory nerve fibers. (**A**) CckGFP_Pgp9.5GFP mice express GFP in CCK-enteroendocrine cells and Pgp9.5 sensory nerve fibers. The two cell types are shown in the enlarged view, with the CCK-enteroendocrine cell represented by a triangle. (**B**) Confocal microscopy image of proximal small intestine villus showing a GFP-labeled CCK-enteroendocrine cell and GFP-labeled Pgp9.5 nerve fibers; 18.9 ± 2.0% SEM of CckGFP cells contact Pgp9.5 fibers (n = 3 mice, >100 cells per mouse). (**C**) PYY-stained enteroendocrine cells (left, green) in the colon contact Phox2b vagal nerve fibers (center, red) in a Phox2bCRE_tdTomato mouse; merged image is shown on the right. (**D**) Two-thirds of CckGFP (green) enteroendocrine cells colocalize with the presynaptic marker synapsin-1 (purple) (n = 6 mice, 200 cells per mouse). (**E**) Real-time quantitative polymerase chain reaction (qPCR) expression levels of presynaptic transcripts, including genes encoding for synaptic adhesion proteins (n = 3 mice, >10,000 cells per cell type per mouse; error bars indicate mean ± SEM; a.u., arbitrary units; EEC, enteroendocrine cell). All scale bars, 10 μm.

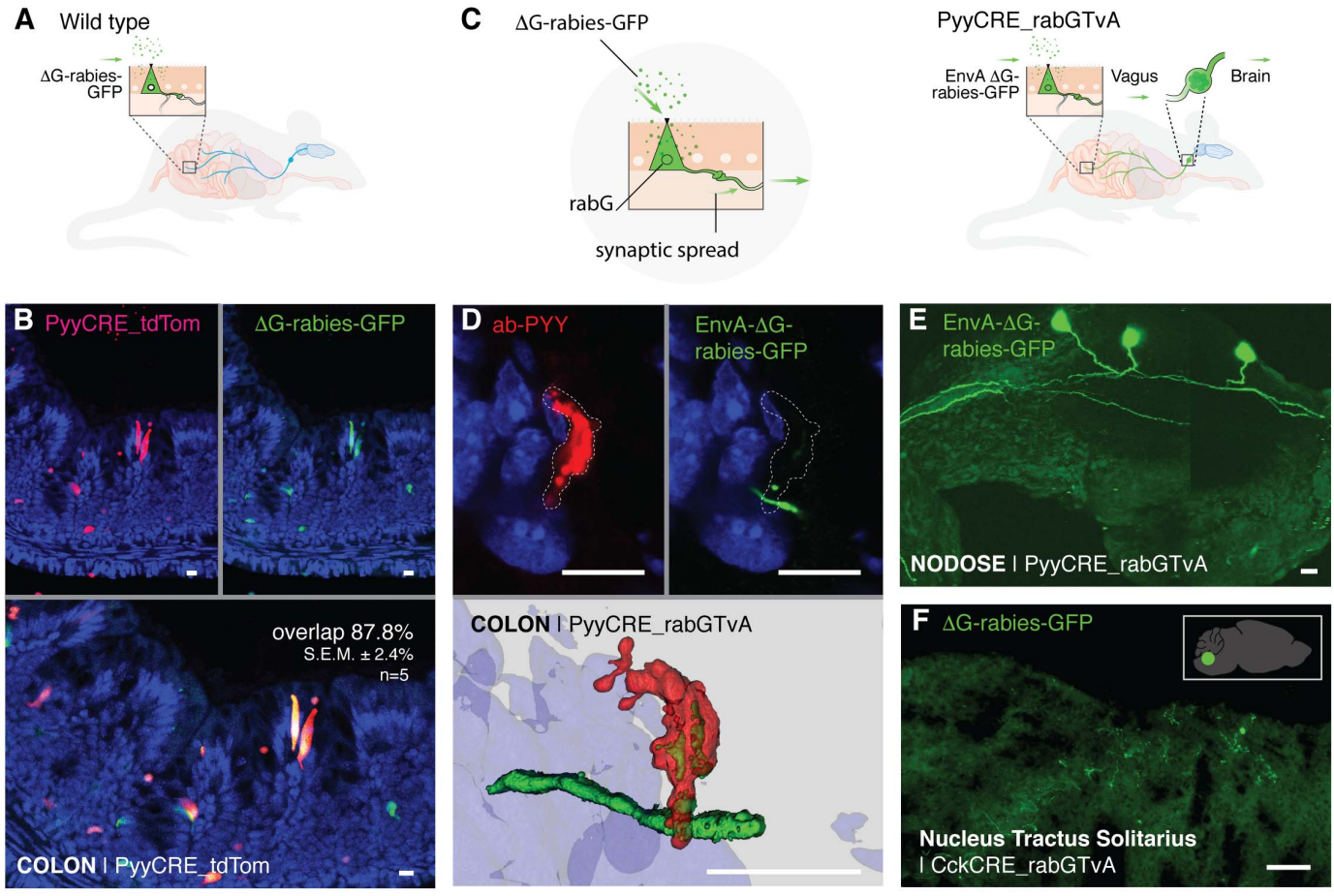

Fig. 2. Enteroendocrine cells of the colon and small intestine synapse with vagal nodose neurons. (**A**) Model of ΔG-rabies-GFP enema delivery. (**B**) PYY cells expressing tdTomato (top left, red) are infected by ΔG-rabies-GFP (top right, green). Overlay (bottom) shows overlap of 87.8 ± 2.4% SEM (n = 5 mice). In the absence of G glycoprotein (ΔG), ΔG-rabies-GFP does not spread beyond the infected PYY cell. (**C**) EnvA-ΔG-rabies-GFP virus enters cells via the TvA receptor and spreads by using the rabG protein within specific cells. (**D**) EnvA-ΔG-rabies-GFP (top right, green) infects PYY cells (top left, red) and spreads synaptically to underlying colon nerve fibers. Three-dimensional reconstruction (bottom) shows EnvA-ΔG-rabies-GFP–infected PYY cell and monosynaptically labeled nerve fiber. (**E**) EnvA-ΔG-rabies-GFP enema infects colonic enteroendocrine cells and spreads onto vagal neurons in the nodose ganglion (green). (**F**) In additional experiments, ΔG-rabies-GFP delivered by oral gavage spreads in the intestinal lumen of CckCRE_rabG-TvA mice to label the nucleus tractus solitarius (green). This neuroepithelial circuit links the intestinal lumen with the brainstem. The inset shows the location of the nucleus tractus solitarius in the mouse brain. All scale bars, 10 μm.

PYY. In the mouse small intestine and colon, enteroendocrine cells contacted sensory nerve fibers (Fig. 1, A to C). About one in five CCK-expressing enteroendocrine (CCK-enteroendocrine) cells contacted Pgp9.5 sensory nerve fibers that express green fluorescent protein (Pgp9.5GFP nerve fibers) (18.9 ± 2.0% SEM, >100 cells per mouse, n = 3 mice) (Fig. 1B). CCK-enteroendocrine cells immunoreact with an antibody against the presynaptic protein synapsin-1 (Fig. 1D), showing that these connections have synaptic features. Furthermore, using single-cell Western blot, we found that 83% of enteroendocrine cells contain synapsin-1 (164 of 198 CckGFP cells analyzed) (fig. S1). Compared with other intestinal epithelial cells, purified CCK-enteroendocrine cells express the synaptic adhesion genes *Efnb2*, *Lrrtm2*, *Lrrc4*, and *Nrxn2* (Fig. 1E), showing that these epithelial sensors have the machinery to form synapses.

From gut lumen to brainstem in one synapse

To determine the source of neurons synapsing with enteroendocrine cells, we used a modified rabies virus (ΔG-rabies-GFP) (*10*). This rabies virus infects neurons but lacks the G glycoprotein necessary for transsynaptic spread (Fig. 2A) (*14*). In intestinal organoids, rabies prefers to infect enteroendocrine cells over other epithelial cells (fig. S2A). In the mouse, when introduced into the lumen of the colon by enema, almost 9 out of 10 infected cells are PYY-enteroendocrine cells (87.8 ± 2.4% SEM, n = 5 mice) (Fig. 2B) (*10*). The lack of fluorescence in the underlying mucosa shows that, in the absence of its G glycoprotein, the rabies virus does not spread beyond infected enteroendocrine cells.

To trace the neural circuit, we bred a mouse (strain PyyCRE_rabG-TvA) in which enteroendocrine cells express the G glycoprotein (rabG) (Fig. 2C). In these mice, rabies delivered by enema infects enteroendocrine cells and spreads through synapses onto nerves. Some of the nerve fibers can be traced to vagal nodose neurons (control group: 0 positive out of 3 PyyCRE_tdTomato mice; experimental group: 4 positive out of 5 PyyCRE_rabG-TvA mice). Furthermore, an enema of the chemical tracer dye Fast Blue labeled both nodose ganglia, confirming that the vagus indeed innervates the distal colon (*15*). In control experiments in which the right cervical vagus was severed, the Fast Blue enema labeled the left (intact) but not the right (vagotomized) nodose (fig. S3).

Because ΔG-rabies-GFP can infect any neuronal cell it contacts, we restricted its entrance to enteroendocrine cells only by using an EnvA-coated rabies (EnvA-ΔG-rabies-GFP) (Fig. 2C). EnvA is an envelope glycoprotein of the avian sarcoma leukosis virus that binds to the avian

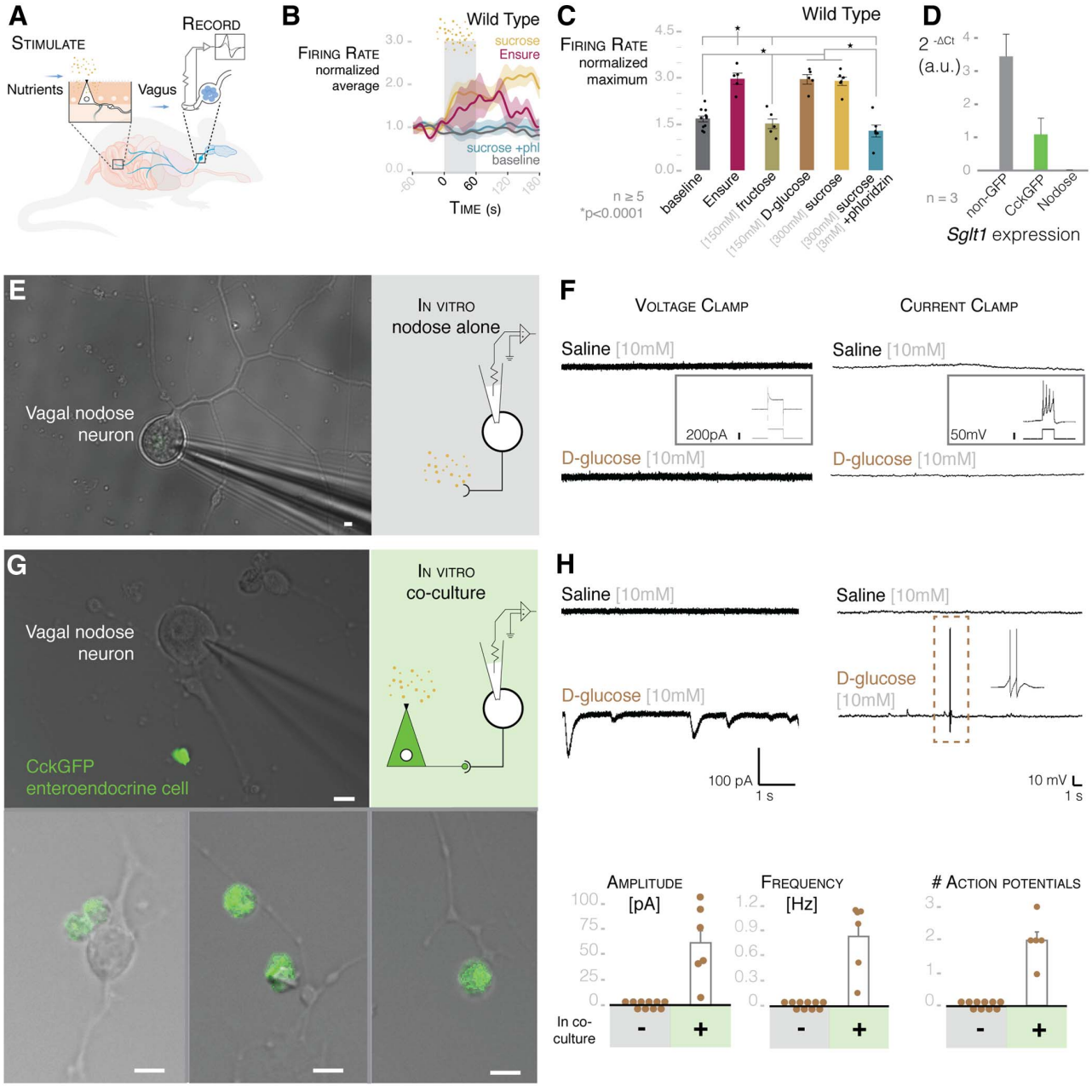

Fig. 3. Enteroendocrine cells transduce glucose stimuli onto vagal neurons. (**A**) Model of intestinal intraluminal perfusion and vagal nerve electrophysiology. (**B**) Normalized traces for baseline, Ensure, 300 mM sucrose, and 300 mM sucrose with 3 mM phloridzin (phl) in wild-type mice. Gray bar indicates treatment period; shading indicates SEM. (**C**) Ensure, 300 mM sucrose, and 150 mM D-glucose stimulate vagal firing rate, which is abolished by SGLT1-blocker phloridzin [$n \geq 5$ mice; *$P < 0.0001$, analysis of variance (ANOVA) with post hoc Tukey's HSD test; error bars indicate SEM]. (**D**) Intestinal epithelial cells express *Sglt1*, but nodose neurons do not ($n = 3$ mice, >10,000 cells per cell type per mouse; data are presented as mean ± SEM). (**E**) Nodose neurons cultured alone for electrophysiology (widefield microscopy image on left, model on right). (**F**) Nodose neurons do not respond to 10 mM glucose in voltage-clamp (left trace) or current-clamp (right trace) mode. Insets show that neurons respond to voltage or current pulse, indicating viability. (**G**) Nodose neurons cocultured with GFP-positive enteroendocrine cells for electrophysiology (image on left, model on right). Innervated enteroendocrine cells are shown at the bottom. (**H**) In coculture, glucose evoked EPSCs (top left) and action potentials (top right) in connected neurons (scale of current or voltage and time are shown below the traces). Dashed-line box indicates action potentials expanded in right inset. Quantification of EPSC amplitude and frequency (bottom left and center; $n = 21$ neurons alone; $n = 6$ neurons connected to enteroendocrine cells) and action potentials (bottom right; $n = 21$ alone; $n = 5$ neurons connected to enteroendocrine cells) in GFP-negative (–) and -positive (+) cells. All scale bars, 10 μm.

TvA receptor. Therefore, EnvA-ΔG-rabies-GFP only infects cells that express the TvA receptor. In the PyyCRE_rabG-TvA mouse, PYY-enteroendocrine cells express the TvA receptor, and an enema of EnvA-ΔG-rabies-GFP infects enteroendocrine cells exclusively. Then, it spreads to synaptically connected neurons. Of a total of nine mice, five had visible infection of nerve fibers in the colon (Fig. 2D), and two of those five had visible infection in the vagal nodose (Fig. 2E and movie S1; confirmed in vitro in fig. S4). Labeled fibers were also observed in the dorsal root ganglia of four out of the five infected mice (fig. S5). No infection of nerves was observed in littermate controls that lack CRE recombinase ($n = 5$ mice).

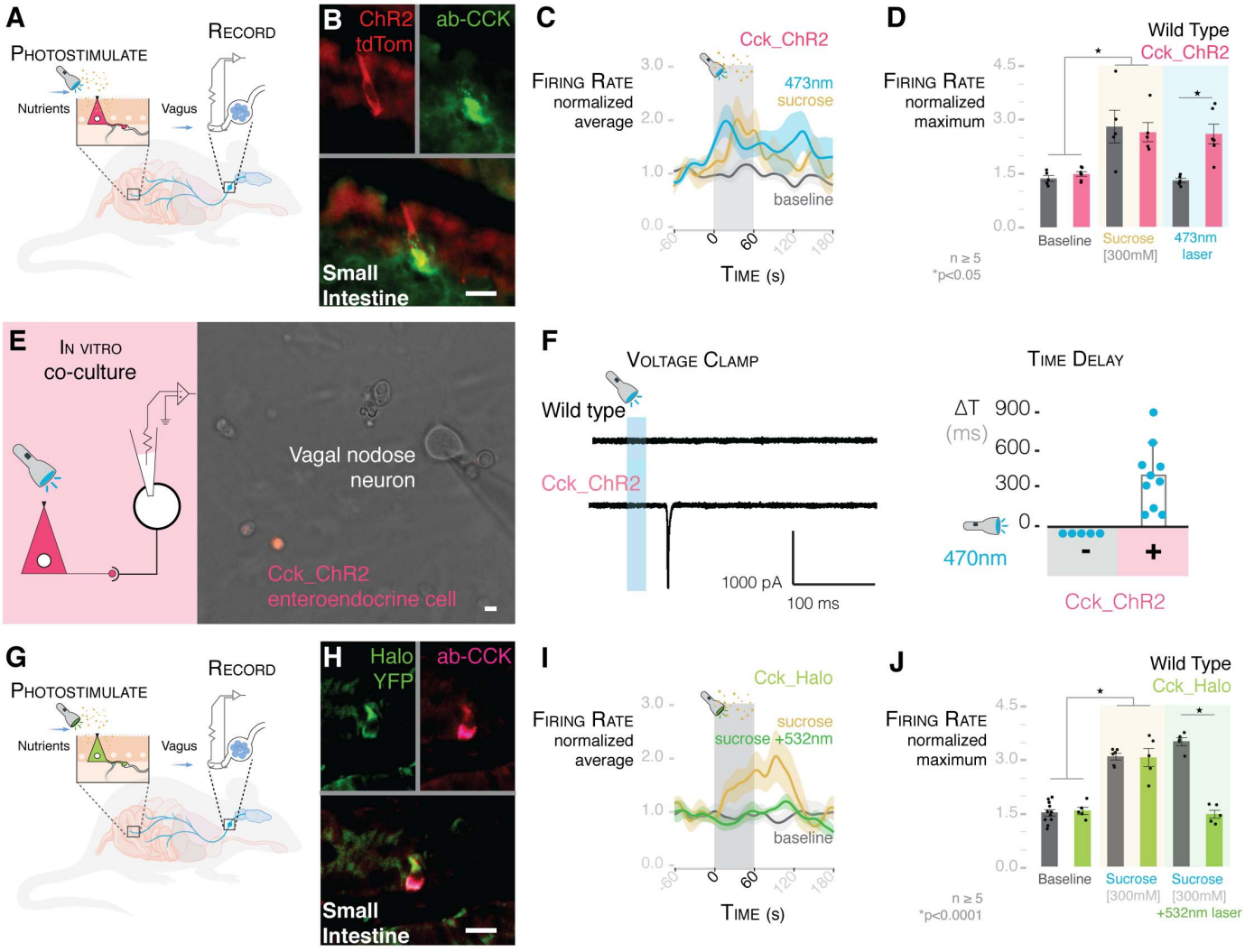

Fig. 4. Millisecond transduction from enteroendocrine cells to vagal neurons. (**A**) Model of intraluminal photostimulation and vagal electrophysiology. (**B**) In CckCRE_ChR2-tdTomato mice, intestinal enteroendocrine cells express ChR2. (**C**) Normalized traces for 473-nm intraluminal laser, 300 mM sucrose, and baseline in CckCRE_ChR2 mice. Shading indicates SEM. (**D**) 473-nm intraluminal laser stimulates vagal firing rate in CckCRE_ChR2, but not wild-type, mice ($n \geq 5$ mice; $^*P < 0.05$, ANOVA with post hoc Tukey's HSD test; error bars indicate SEM). (**E**) Patch-clamp electrophysiology of neurons (model on left) in coculture with CckCRE_ChR2 cells (image on right). (**F**) In coculture, 473-nm photostimulation evoked EPSCs (trace on left) in connected nodose neurons (quantification on right) ($n = 9$ neurons connected to enteroendocrine cells; –, neurons alone; +, neurons cocultured with enteroendocrine cells; ΔT, time between stimulus and onset of EPSCs). Scale of current and time is shown below the trace. (**G**) Model of intraluminal photoinhibition and vagal electrophysiology. (**H**) In CckCRE_Halo-YFP mice, intestinal enteroendocrine cells express halorhodopsin (eNpHR3.0). (**I**) Normalized traces for baseline, 300 mM sucrose, and 300 mM sucrose with 532-nm intraluminal laser. Shading indicates SEM. (**J**) In CckCRE_Halo, but not wild-type, mice, a 532-nm intraluminal laser abolishes the effect of sucrose on vagal firing rate ($n \geq 5$ mice per group; $^*P < 0.0001$, ANOVA with post hoc Tukey's HSD test; error bars indicate SEM). All scale bars, 10 μm.

Delivering the virus by oral gavage into CckCRE_rabG-TvA mice yielded similar results (fig. S5). In these mice, labeled vagal nodose neurons projected upstream into the nucleus tractus solitarius of the brainstem (Fig. 2F). Monosynaptic rabies tracing shows a neural circuit linking the small intestine or colon lumen to the brainstem in one synapse.

A gut-brain neural circuit in a dish

In coculture, vagal nodose neurons clearly extended axons to enteroendocrine cells of intestinal organoids (fig. S4A and movie S2). We traced this neural circuit in vitro using EnvA-ΔG-rabies-GFP to confirm that synapses are formed. To ensure that only infected neurons spread EnvA-ΔG-rabies-GFP, nodose neurons were incubated with virus before coculture with organoids. In control experiments, EnvA-ΔG-rabies-GFP did not infect wild-type nodose neurons (fig. S4B). However, EnvA-ΔG-rabies-GFP infected vagal nodose neurons that express the TvA receptor (Phox2bCRE_rabG-TvA). Forty-eight to 72 hours after coculture, the virus spread onto enteroendocrine cells in intestinal organoids, demonstrating synaptic connection in vitro (fig. S4C).

Transduction of a sense from gut to brain

We tested the function of this neuroepithelial circuit using luminal stimuli and whole-nerve electrophysiology. The initial stimulus used was Ensure—a whole-nutrient solution. Luminal Ensure stimulated an increase in vagal firing rate (Fig. 3, A to C). Next, we focused on a distinctive nutrient, sugar. When ingested, sugar is sensed in the duodenum, but it is unclear whether this stimulus is sensed by the vagus directly or transduced via enteroendocrine cells (*16*). In wild-type mice, perfusing the sugar sucrose (100 to 300 mM) significantly increased vagal firing rate

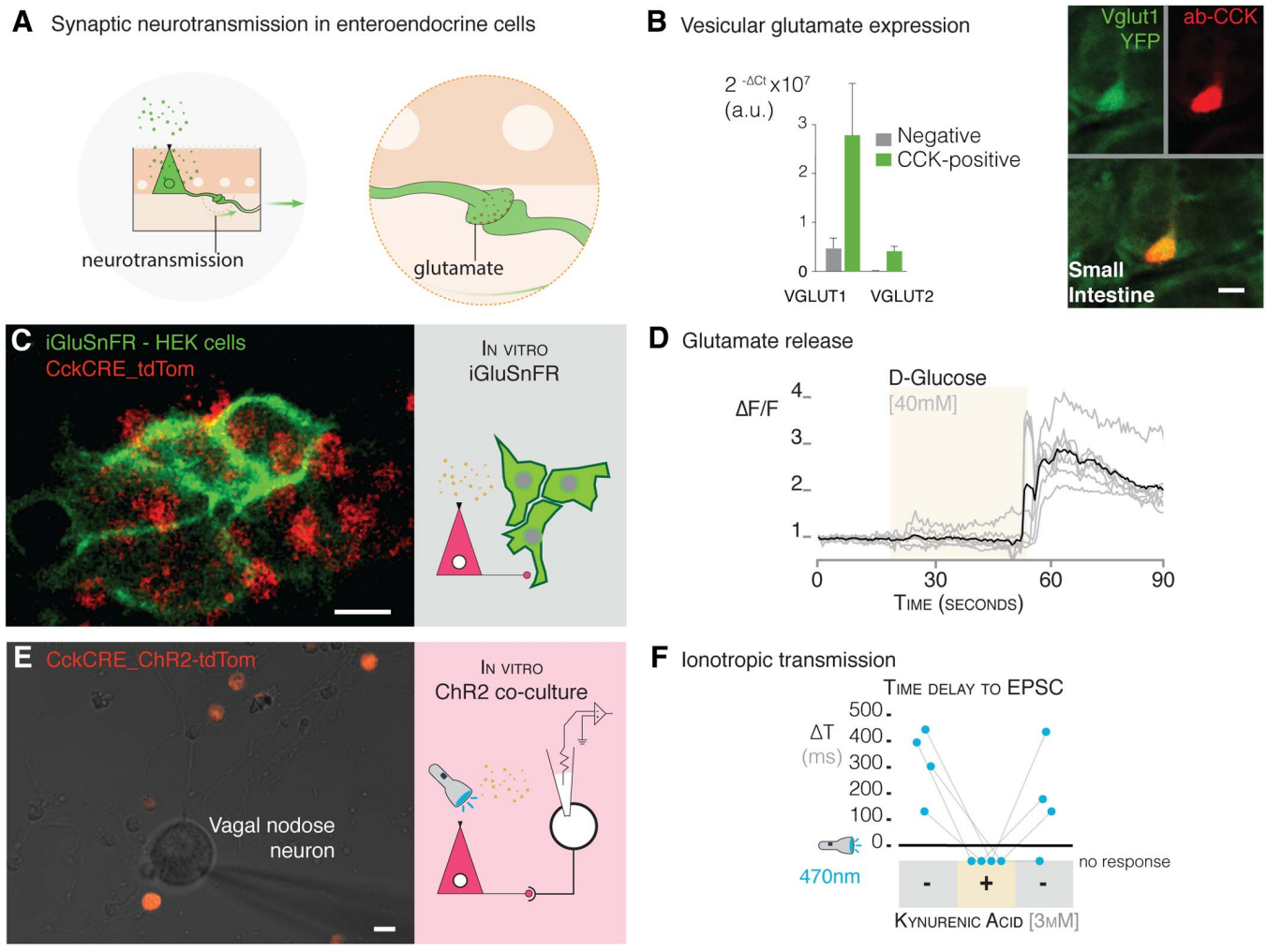

Fig. 5. Glutamate is used as a neurotransmitter between enteroendocrine cells and neurons. (**A**) Model of synaptic neurotransmission in enteroendocrine cells. (**B**) Enteroendocrine cells express the vesicular glutamate genes encoding VGLUT1 and 2 (*Slc17a7* and *Slc17a6*) (quantification by qPCR on left, confocal microscopy images on right). (**C**) CckCRE_tdTomato enteroendocrine cells were cocultured with HEK cells that express the glutamate sniffer protein, iGluSnFR (multiphoton microscopy image on left, model on right). (**D**) A stimulus of 40 mM D-glucose administered during the time period indicated by the beige shading elicits a response in iGluSnFR-HEK cells (n = 3 cultures; individual cell, gray trace; average of all cells, black trace). ΔF/F, difference in fluorescence intensity between resting state and after stimulus. (**E**) Coculture with neurons and CckCRE_ChR2 cells (multiphoton microscopy image on left) for electrophysiology of neurons and microperfusion of the glutamate-receptor blocker kynurenic acid (model on right). (**F**) In coculture, 473-nm photostimulation evoked EPSCs in connected nodose neurons, these currents were abolished, and no response was observed with the addition (+) of 3 mM kynurenic acid. The response was recovered after the drug was washed off (indicated by second "–" condition on right) (n = 4 neurons connected to enteroendocrine cells). All scale bars, 10 μm.

over baseline (Fig. 3, B and C, and fig. S6). D-Glucose (150 mM), but not fructose (150 mM), had the same effect. No effect was observed when the vagus was severed (fig. S7), when hyperosmolar phosphate-buffered saline was perfused (700 mosmol), or when sucrose was applied intraperitoneally (300 mM) (fig. S8). The vagal response was abolished when sucrose was perfused with phloridzin, a blocker of the electrogenic glucose transporter SGLT1 (*17*) (Fig. 3, B and C). A transcription profile showed that, unlike vagal nodose neurons, CCK-enteroendocrine cells express *Sglt1*, suggesting that the stimulus is transduced by the epithelial cells (Fig. 3D).

Evidence gathered on dissociated colonic enteroendocrine cells, and the enteroendocrine-like cell line STC1, has shown that enteroendocrine cells sense glucose (*18*). We therefore packaged a rabies virus to carry the calcium reporter GCaMP6s (ΔG-rabies-GCaMP6s) and used it to infect enteroendocrine cells in intestinal organoids. When presented with D-glucose (10 mM), calcium transients were elicited in CCK-enteroendocrine cells (56.0 ± 20.0% of the KCl control response; n = 3 cells) (fig. S2, B to D). One previous report found that rat nodose neurons respond to glucose (*19*). However, in contrast with enteroendocrine cells, vagal neurons are unlikely to face steep changes in glucose concentrations because they do not contact the intestinal lumen (*20*). We therefore measured calcium transients in dissociated nodose neurons and found that D-glucose (10 mM) did not elicit a response (fig. S9, A and B) (n = 246 cells pooled from three mice).

To discard the possibility that only nodose neurons innervating the intestine may sense glucose, we retrotraced them by injecting Fast Blue dye into the duodenum (fig. S9C). In Fast Blue–labeled vagal neurons, no calcium response was observed in the presence of D-glucose (20 mM) (fig. S9C). Furthermore, neither excitatory currents nor action potentials were observed in the presence of a D-glucose (10 to 20 mM) stimulus using patch-clamp electrophysiology (Fig. 3, E and F). Current injection demonstrated that these cultured nodose neurons were functionally viable (inset of Fig. 3F).

We then cocultured vagal nodose neurons with intestinal enteroendocrine cells (*10*). After 48 to 72 hours, there were visible connections between neurons and enteroendocrine cells (Fig. 3G). Coculturing did not alter the resting membrane potential, the current, or the spike threshold of the vagal nodose neurons. However, a D-glucose (10 mM) stimulus now evoked excitatory postsynaptic currents (EPSCs) and action potentials in those neurons connected to enteroendocrine cells (Fig. 3H). In voltage-clamp mode, the average current of the EPSCs was 61.65 ± 15.21 pA, and the average frequency was 0.86 ± 0.17 Hz (n = 6 neurons connected to enteroendocrine cells). In current-clamp mode, this in vitro connection was sufficient to elicit action potentials in the connected neurons (average of 2 ± 0.32 action potentials, n = 5 neurons connected to enteroendocrine cells).

Synaptic speed and specificity

Two recent reports have shown that hypothalamic neurons controlling food intake are inhibited by nutrients within seconds of the nutrients entering the duodenum (*21*, *22*). Therefore, it is likely that enteroendocrine cells transduce sensory signals from nutrients at a much faster rate than previously thought possible. To test the speed of transduction, we bred a mouse (strain CckCRE_ChR2-tdTomato) in which enteroendocrine cells express channelrhodopsin 2 (ChR2) —an excitatory light-gated ion channel activated by 473-nm light (Fig. 4, A and B). A 473-nm stimulus applied to these cells elicited excitatory currents and significantly reduced food intake by the mice, showing functional expression of the channel (fig. S10) (see methods).

Vagal firing rate is significantly increased when a 473-nm laser stimulus is applied to the duodenal lumen of CckCRE_ChR2 mice. No response was observed in wild-type controls (Fig. 4, C and D; for laser-activation controls, see fig. S11). The firing rate increased rapidly after laser stimulation, reaching its peak, on average, in 72.7 ± 20.9 s (fig. S12). In vitro, vagal nodose neurons cultured alone did not respond to photostimulation. To determine the precise transduction speed, we cocultured them with CckCRE_ChR2 enteroendocrine cells (Fig. 4E). In vagal nodose neurons connected to enteroendocrine cells, a 470-nm photostimulus elicited EPSCs within 60 to 800 ms (n = 9 pairs) (Fig. 4F).

To test the specificity of transduction, we bred a mouse (CckCRE_Halo-YFP) in which intestinal enteroendocrine cells express the light-inhibitory channel eNpHR3.0 (halorhodopsin)—an inhibitory light-gated ion channel activated by 532-nm light (Fig. 4, G and H)—and yellow fluorescent protein (YFP). In these mice, luminal sucrose (300 mM) elicited a vagal response; however, when a 532-nm laser stimulus was presented along with the sucrose, vagal activity was abolished (Fig. 4, I and J; for laser activation controls, see fig. S13). In control wild-type mice, a 532-nm laser stimulus failed to attenuate the sucrose response. These data revealed that enteroendocrine cells are necessary and sufficient to transduce a glucose stimulus onto vagal neurons within milliseconds.

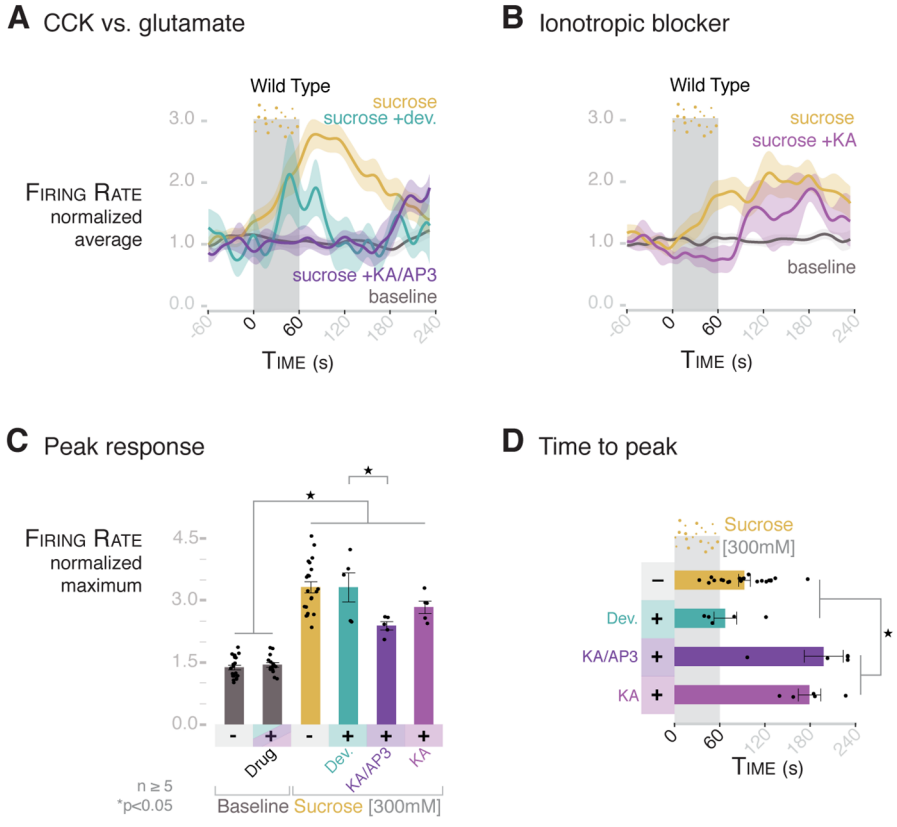

Fig. 6. The rapid vagal response to sucrose is dependent on glutamate, whereas CCK contributes to the prolonged response. (**A**) Normalized traces for baseline, 300 mM sucrose, 300 mM sucrose after treatment with 2 mg/kg devazepide, and 300 mM sucrose after treatment with glutamate inhibitor cocktail KA/AP3 [150 μg/kg kynurenic acid (KA) with 1 mg/kg DL-2-amino-3-phosphonoproprionic acid (AP-3)] in wild-type mice. Shading indicates SEM. (**B**) Normalized traces for baseline, 300 mM sucrose, and 300 mM sucrose after treatment with 150 μg/kg KA in wild-type mice. Shading indicates SEM. (**C**) KA/AP3 attenuates the maximum normalized vagal firing rate in response to sucrose, whereas devazepide and KA alone do not. (**D**) KA/AP3 and KA alone prolong the time to peak from an average of 92.8 s to 198 and 179 s, respectively. Devazepide (2 mg/kg) does not significantly change the time to peak (mean = 67.1 s). For (C) and (D), $n \geq 5$ mice per group; *$P < 0.05$, ANOVA with post hoc Tukey's HSD test; error bars indicate SEM.

The neurotransmitter

The possibility exists that innervated enteroendocrine cells could use a classic neurotransmitter to transduce the above-described sensory signals. Other sensory epithelial transducers—including photoreceptors (*23*), auditory hair cells (*24*), Merkel cells (*25*), and olfactory receptor cells (*26*)—use vesicular glutamate as a neurotransmitter. Thus, we hypothesized that enteroendocrine cells use glutamate as a neurotransmitter as well. We found that intestinal enteroendocrine cells express significant quantities of the transcript for the vesicular glutamate transporter 1 protein (VGLUT1) (Fig. 5, A and B). In a transgenic Vglut1CRE_YFP mouse, fluorescence was observed in distinct intestinal epithelial cells that resemble enteroendocrine cells, and almost 4 in 10 of those fluorescent cells costained for CCK (38.80 ± 2.53% SEM, 100 cells per mouse, n = 3 mice). Moreover, vagal nodose neurons express at least eight glutamate receptors (fig. S14).

To test whether enteroendocrine cells release glutamate, we used the sniffer protein iGluSnFR. This membrane-bound protein fluoresces green in the presence of glutamate (*27*). Transfected iGluSnFR–HEK (human embryonic kidney) cells did not respond to a D-glucose (40 mM) stimulus but did respond to glutamate (100 μM) (fig. S15). We then cocultured iGluSnFR-HEK cells with Tomato-expressing enteroendocrine cells (CckCRE_tdTomato) (Fig. 5C). This time, when presented with a D-glucose stimulus (40 mM), iGluSnFR-HEK cells fluoresced green (n = 3 cultures; Fig. 5D), indicating that enteroendocrine cells release glutamate. Then, we cocultured CckCRE_ChR2 enteroendocrine cells with vagal neurons to determine if glutamate serves as a neurotransmitter in this synapse. In connected neurons, a 470-nm stimulus elicited EPSCs that were abolished by adding kynurenic acid (3 mM), an ionotropic glutamate-receptor

blocker (Fig. 5, E and F). The response was recovered once the blocker was washed away (n = 4 neurons connected to enteroendocrine cells) (Fig. 5F).

Hormone versus neurotransmitter

In a transgenic mouse in which VGLUT1-enteroendocrine cells express ChR2 (Vglut1CRE_ChR2-YFP), a luminal laser stimulus of 473-nm significantly increased vagal firing rate (fig. S16). The amplitude and timing of the peak response was comparable to the CckCRE_ChR2 experiments (figs. S12 and S16). The same laser stimulus applied to the subdiaphragmatic or cervical vagus did not alter firing rate (fig. S17). However, the response was abolished when the 473-nm laser was presented along with a cocktail of glutamate-receptor blockers [metabotropic blocker AP-3 (1 mg per kg of body weight) with ionotropic blocker kynurenic acid (150 μg/kg)] (fig. S16). These data revealed a type of enteroendocrine cell that uses glutamate to drive vagal firing.

Next, we compared the respective contributions of CCK and glutamate to vagal firing. The peak vagal firing rate elicited by a sucrose stimulus was not affected when the CCK-A receptor was blocked with devazepide (2 mg/kg) (Fig. 6, A and C). In control experiments, the same dose of devazepide fully blocked the vagal response to luminal CCK (fig. S18). Although the peak response and time to peak were not altered by devazepide, the length of the response was attenuated after 120 s (Fig. 6, A, C, and D; and figs. S18 and S19), suggesting that it takes minutes for released CCK to stimulate vagal firing. By contrast, blocking both ionotropic and metabotropic glutamate receptors attenuated the speed, peak, and magnitude of the vagal response to sucrose (Fig. 6, C and D, and fig. S19). Indeed, the first 60 s of the vagal response to sucrose was suppressed by the ionotropic blocker kynurenic acid alone (Fig. 6B and fig. S20), delaying the time to peak to around 180 s (Fig. 6D and fig. S18C). These data revealed that synaptic glutamate is used by an epithelial sensor cell in the gut to rapidly transduce luminal stimuli to the central nervous system.

The neuropod cells

In recent years, enteroendocrine cells have emerged as sensors of mechanical, chemical, and bacterial signals in the gastrointestinal tract (*2*, *3*). However, their transducer properties have been obscured by their name. By synapsing with the vagus, these sensor cells provide a neuroepithelial circuit for fast sensory transduction. As such, we see the need for a new name to refer to gut sensory epithelial cells that synapse with nerves. We refer to these cells as neuropod cells. We hypothesize that the gut-brain neural circuit formed by neuropod cells and vagal nodose neurons could lead to the following possibilities: (i) rapid computation of stimuli to distinguish their physical (e.g., volume) versus chemical (e.g., calorie) properties; (ii) precise sensory representation of specific gastrointestinal regions; (iii) localized plasticity encoded within the neural circuit; and (iv) timely vagal efferent feedback to modulate gastrointestinal sensory function. Like other sensory transducers, neuropod cells use synaptic signals to help the brain make sense of the food we eat.

Materials and methods summary

Animals

Mouse care and experiments were carried out in accordance with protocols approved by the Institutional Animal Care and Use Committee at Duke University Medical Center under the protocol A009-16-01. Mice were housed in the Duke University animal facilities, where they were kept on a 12-hour light-dark cycle. They received food and water ad libitum. The specific strains can be found in the supplemental methods.

Rabies production and tracing

G-deleted rabies virus production was performed in house as described in Wickersham *et. al* (*28*). For colon monosynaptic tracing, P1 mice were given an enema of EnvA-ΔG-rabies-GFP (5.9×10^9 ffu/ml). For small intestine monosynaptic tracing, P1 mice were given a gavage of ΔG-rabies-GFP (9.8×10^8 ffu/ml). Mice were sacrificed 7 days after exposure at P8. Harvested tissue was fixed in 4% PFA then treated with serial sucrose solutions. Ganglia were whole-mount imaged with a multiphoton microscopy system (Bruker Ultima IV with a Chameleon Vision II tunable laser). All other tissue was frozen in OCT blocks and sectioned for immunohistochemistry.

Organoid culture

Organoids were cultured using a protocol adapted from Sato *et al.* 2009 (*29*). Isolated crypts were resuspended in Matrigel (Corning #356231) and plated 50 μl per well in a 24-well plate in organoid media. Organoid media contains 1x Glutamax, 10 10mM HEPES, 200 U/ml Penicillin-Streptomycin, 1× N2 supplement, 1× B27 supplement, 0.25 ng/ml EGF, 50 ng/ml Noggin, and 100 ng/ml r-Spondin in Advanced DMEM/f12.

Enteroendocrine cell and nodose neuron coculture

Enteroendocrine cells of CckGFP and CckCRE_ChR2-tdTomato small intestines were isolated as previously described in Bohórquez *et al.* (*10*). Enteroendocrine cells were sorted into organoid culture media (listed above) plus 10 ng/ml NGF. Sorted cells were plated on 1% Matrigel coated 12-mm coverslips at a concentration of ~5000 to 10,000 enteroendocrine cells per coverslip. Nodose neurons were dissected and incubated with Liberase (Roche) digestion enzyme. Neurons in media were plated evenly on up to eight coverslips with enteroendocrine cells. Patch-clamp electrophysiology was performed 2 to 5 days after plating.

Immunohistochemistry

Immunohistochemistry was performed as previously described in Bohórquez *et al.* (*10*). Primary antibodies: Rb-Anti-PYY [DVB3] (1:1000); Rb-Anti-CCK (1:1000; courtesy of Rodger Liddle or Phoenix Pharmaceuticals H-069-04); Gt-Anti-PSD95 (1:500; Santa Cruz Biotechnology: sc-6926); Rb-Anti-Syn1 (1:500; Cell Signaling Technology: 5297S); Ck-Anti-GFP (1:500; Abcam: ab13970]. Secondary antibodies from Jackson Immuno-Reseach: Dk-Anti-Rb-488 (1:250); Dk-Anti-Rb-Cy3 (1:250); Dk-Anti-Gt-Cy5 (1:250); and Dk-Anti-Ck-488 (1:250). Imaging was done on a Zeiss 880 Airyscan inverted confocal microscope. Data are presented as the mean percentage ± SEM.

Real-time quantitative PCR

RNA from CckGFP-positive and -negative epithelial cells was extracted based on the manufacturer's protocol using the RNeasy Micro Plus Kit (Qiagen #74034). Then cDNA was produced per manufacturer's protocol using the High Capacity cDNA Reverse Transcription Kit (Applied Biosystems #4368814). TaqMan probes used are listed in supplemental materials. Real-time qPCR was run on a StepOnePlus System (Thermo Fischer), using TaqMan Fast Universal PCR Master Mix (Applied Biosystems #4352042) according to the manufacturer's protocol. Transcription rate was determined as $2^{-\Delta Ct}$, or compared as fold-change over GFP negative epithelial cells using $2^{-\Delta\Delta Ct}$. All values are reported as mean ± SEM.

Electrophysiology

Enteroendocrine cells and nodose neurons were cocultured as described above. Recordings were carried out at room temperature using a MultiClamp 700B amplifier (Axon Instruments), digitized using a Digidata 1550A (Axon Instruments) interface, and pClamp software (Axon Instruments) for data acquisition. Recordings were made using borosilicate glass pipettes pulled to ~3.5 MΩ resistance. Extracellular solution contained (in mM): 140 NaCl, 5 KCl, 2 CaCl2, 2 MgCl2, 10 HEPES, pH 7.4 (300 to 305 mosmol). For voltage-clamp recordings, intracellular solution contained (in mM): 140 CsF, 10 NaCl, 0.1 CaCl2, 2 MgCl2, 1.1 EGTA, 10 HEPES, 10 sucrose (pH 7.25, 290 to 295 mosmol). For current-clamp recordings, intracellular solution contained (in mM): 140 KCl, 0.5 EGTA, 5 HEPES, 3 Mg-ATP, 10 sucrose (pH 7.25, 290 to 295 mosmol). Data are presented as the mean ± SEM, and significance was determined using a two-tailed Student's t test.

iGluSnFR-HEK cell and enteroendocrine cell coculture and imaging

CckCRE_tdTomato enteroendocrine cells were isolated as described above. Isolated cells were mixed with iGluSnFR-HEK cells at a ratio of 10:1, then plated on 1% Matrigel coated coverslips. Control iGluSnFR-HEK cells were plated alone. Cells were incubated for 12 to 18 hours before imaging. Coverslips were imaged using a multiphoton microscopy system (Bruker Ultima IV with a Chameleon Vision II tunable laser). Imaging series were analyzed using Fiji (it's just ImageJ), and cell traces were plotted with Excel.

Vagus nerve recording

Wild-type control (n = 5 to 9), CckCRE_ChR2-tdTomato (n = 6), CckCRE_Halo-YFP (n = 5), and Vglut1CRE_ChR2-YFP (n = 6) mice were used for vagal recordings. The cervical vagus was exposed in anesthetized mice and two platinum iridium wires (Medwire by Sigmund Cohn Corp) were looped around the vagus nerve for recording. A 20-gauge gavage needle was surgically inserted through the stomach wall and into the duodenum. Saline and stimulant tubes were connected to the gavage needle. For optogenetic experiments, a fiber optic cable (FT020, ThorLabs) was threaded through the gavage needle into the lumen of the duodenum. A perfusion exit incision was made 10 cm distal to the pyloric sphincter. During each recording, PBS was constantly perfused through the duodenum using a peristaltic pump (Cole-Parmer) at the lowest setting for a flow rate of ~400 µl PBS per minute. For stimulus delivery, see extended methods in supplemental materials. Data acquisition: A differential amplifier and bandpass filter (1000× gain, 300-Hz to 5-kHz bandpass filter; A-M Systems LLC) was used and the signal was processed using a data acquisition board and software (20-kHz sampling rate; Signal Express, National Instruments Corp). The raw data was analyzed using a spike sorting algorithm (MATLAB by MathWorks). Spikes were detected using simple threshold detection based on RMS noise. The firing rate was calculated using a Gaussian kernel smoothing algorithm (200-ms time scale). Statistical Methods: Stimulation response was quantified as the maximum firing rate after stimulation (stimulant conditions) or during recording (baseline). Time to peak was calculated as time from start of stimulus to maximum firing rate. Area under the curve was calculated as area under the curve for the entire 6-min recording. Maximum firing rate, time to peak, and area under curve are analyzed across genotype, stimulation condition, and their interaction term by ANOVA, followed by Tukey HSD post hoc testing (JMP by SAS Institute).

REFERENCES AND NOTES

1. B. Alberts, D. Bray, J. Lewis, M. Raff, K. Roberts, J. D. Watson, *Molecular Biology of the Cell* (Garland, ed. 3, 1994), pp. 907–982.
2. A. Psichas, F. Reimann, F. M. Gribble, Gut chemosensing mechanisms. *J. Clin. Invest.* **125**, 908–917 (2015). doi: 10.1172/JCI76309; pmid: 25664852
3. J. B. Furness, L. R. Rivera, H. J. Cho, D. M. Bravo, B. Callaghan, The gut as a sensory organ. *Nat. Rev. Gastroenterol. Hepatol.* **10**, 729–740 (2013). doi: 10.1038/nrgastro.2013.180; pmid: 24061204
4. F. Feyrter, *Über diffuse endokrine epitheliale Organe* (J. A. Barth, Leipzig, Germany, 1938).
5. J. F. Rehfeld, The new biology of gastrointestinal hormones. *Physiol. Rev.* **78**, 1087–1108 (1998). doi: 10.1152/physrev.1998.78.4.1087; pmid: 9790570
6. D. Castaneda *et al*., Mechanosensitive ION channel Piezo2 distribution in mouse small bowel and colon enterochromaffin cells. *Gastroenterology* **152**, S180 (2017). doi: 10.1016/S0016-5085(17)30916-2
7. T. Braun, P. Voland, L. Kunz, C. Prinz, M. Gratzl, Enterochromaffin cells of the human gut: Sensors for spices and odorants. *Gastroenterology* **132**, 1890–1901 (2007). doi: 10.1053/j.gastro.2007.02.036; pmid: 17484882
8. H. J. Jang *et al*., Gut-expressed gustducin and taste receptors regulate secretion of glucagon-like peptide-1. *Proc. Natl. Acad. Sci. U.S.A.* **104**, 15069–15074 (2007). doi: 10.1073/pnas.0706890104; pmid: 17724330
9. G. J. Rogers *et al*., Electrical activity-triggered glucagon-like peptide-1 secretion from primary murine L-cells. *J. Physiol.* **589**, 1081–1093 (2011). doi: 10.1113/jphysiol.2010.198069; pmid: 21224236
10. D. V. Bohórquez *et al*., Neuroepithelial circuit formed by innervation of sensory enteroendocrine cells. *J. Clin. Invest.* **125**, 782–786 (2015). doi: 10.1172/JCI78361; pmid: 25555217
11. N. W. Bellono *et al*., Enterochromaffin cells are gut chemosensors that couple to sensory neural pathways. *Cell* **170**, 185–198.e16 (2017). doi: 10.1016/j.cell.2017.05.034; pmid: 28648659
12. A. L. Haber *et al*., A single-cell survey of the small intestinal epithelium. *Nature* **551**, 333–339 (2017). doi: 10.1038/nature24489; pmid: 29144463
13. L. L. Glass *et al*., Single-cell RNA-sequencing reveals a distinct population of proglucagon-expressing cells specific to the mouse upper small intestine. *Mol. Metab.* **6**, 1296–1303 (2017). doi: 10.1016/j.molmet.2017.07.014; pmid: 29031728
14. N. R. Wall, I. R. Wickersham, A. Cetin, M. De La Parra, E. M. Callaway, Monosynaptic circuit tracing in vivo through Cre-dependent targeting and complementation of modified rabies virus. *Proc. Natl. Acad. Sci. U.S.A.* **107**, 21848–21853 (2010). doi: 10.1073/pnas.1011756107; pmid: 21115815
15. S. M. Altschuler, J. Escardo, R. B. Lynn, R. R. Miselis, The central organization of the vagus nerve innervating the colon of the rat. *Gastroenterology* **104**, 502–509 (1993). doi: 10.1016/0016-5085(93)90419-D; pmid: 8425692
16. E. K. Williams *et al*., Sensory neurons that detect stretch and nutrients in the digestive system. *Cell* **166**, 209–221 (2016). doi: 10.1016/j.cell.2016.05.011; pmid: 27238020
17. A. Sclafani, H. Koepsell, K. Ackroff, SGLT1 sugar transporter/sensor is required for post-oral glucose appetition. *Am. J. Physiol. Regul. Integr. Comp. Physiol.* **310**, R631–R639 (2016). doi: 10.1152/ajpregu.00432.2015; pmid: 26791832
18. F. Reimann *et al*., Glucose sensing in L cells: A primary cell study. *Cell Metab.* **8**, 532–539 (2008). doi: 10.1016/j.cmet.2008.11.002; pmid: 19041768
19. G. Grabauskas, I. Song, S. Zhou, C. Owyang, Electrophysiological identification of glucose-sensing neurons in rat nodose ganglia. *J. Physiol.* **588**, 617–632 (2010). doi: 10.1113/jphysiol.2009.182147; pmid: 20008464
20. H. R. Berthoud, M. Kressel, H. E. Raybould, W. L. Neuhuber, Vagal sensors in the rat duodenal mucosa: Distribution and structure as revealed by in vivo Dil-tracing. *Anat. Embryol. (Berl.)* **191**, 203–212 (1995). doi: 10.1007/BF00187819; pmid: 7771683
21. L. R. Beutler *et al*., Dynamics of gut-brain communication underlying hunger. *Neuron* **96**, 461–475.e5 (2017). doi: 10.1016/j.neuron.2017.09.043; pmid: 29024666
22. Z. Su, A. L. Alhadeff, J. N. Betley, Nutritive, post-ingestive signals are the primary regulators of AgRP neuron activity. *Cell Reports* **21**, 2724–2736 (2017). doi: 10.1016/j.celrep.2017.11.036; pmid: 29212021
23. C. Brandon, D. M. Lam, L-glutamic acid: A neurotransmitter candidate for cone photoreceptors in human and rat retinas. *Proc. Natl. Acad. Sci. U.S.A.* **80**, 5117–5121 (1983). doi: 10.1073/pnas.80.16.5117; pmid: 6136039
24. O. P. Ottersen *et al*., Molecular organization of a type of peripheral glutamate synapse: The afferent synapses of hair cells in the inner ear. *Prog. Neurobiol.* **54**, 127–148 (1998). doi: 10.1016/S0301-0082(97)00054-3; pmid: 9481795
25. H. Haeberle *et al*., Molecular profiling reveals synaptic release machinery in Merkel cells. *Proc. Natl. Acad. Sci. U.S.A.* **101**, 14503–14508 (2004). doi: 10.1073/pnas.0406308101; pmid: 15448211
26. D. A. Berkowicz, P. Q. Trombley, G. M. Shepherd, Evidence for glutamate as the olfactory receptor cell neurotransmitter. *J. Neurophysiol.* **71**, 2557–2561 (1994). doi: 10.1152/jn.1994.71.6.2557; pmid: 7931535
27. J. S. Marvin *et al*., An optimized fluorescent probe for visualizing glutamate neurotransmission. *Nat. Methods* **10**, 162–170 (2013). doi: 10.1038/nmeth.2333; pmid: 23314171
28. I. R. Wickersham *et al*., Monosynaptic restriction of transsynaptic tracing from single, genetically targeted neurons. *Neuron* **53**, 639–647 (2007). doi: 10.1016/j.neuron.2007.01.033; pmid: 17329205
29. T. Sato *et al*., Single Lgr5 stem cells build crypt-villus structures in vitro without a mesenchymal niche. *Nature* **459**, 262–265 (2009). doi: 10.1038/nature07935; pmid: 19329995

ACKNOWLEDGMENTS

The authors wish to thank Y. H. Kim, A. Chamessian, M. Park, S. Swain, M. Foster, C. Chen, W. Liu, and G. Wen for their contributions. We also thank A. Pereda, R. Liddle, S. Lisberger, E. Bohórquez, and the Grass Laboratory and Grass Fellows classes of '14, '16, and '17 for their constructive feedback. We thank L. Looger for his gracious donation of the iGluSnfR plasmid. Our sincere appreciation is expressed to the staff of the Duke Light Microscopy and Flow Cytometry Core Facilities. The laboratory mailing address is MSRB-I, room 221A, 203 Research Drive, Durham, NC 27710, USA. **Funding:** NIH K01 DK-103832 (PI, D.V.B.), NIH R03 DK114500-01 (PI, D.V.B.), AGA-Elsevier Pilot Research Award (PI, D.V.B.), NIH P30 DK034987 UNC-CGIBD Pilot Research Award (PI, D.V.B.), DARPA-ElectRx N2002850300 (PI, X.S.; Co-I, D.V.B.), NIH 1OT2OD023849-01 (PI, X.S.; Co-I, D.V.B.), The Hartwell Foundation (PI, D.V.B.), The Dana Foundation (PI, D.V.B.), and The Grass Foundation (PI, D.V.B.). K.L.B. is a Howard Hughes Medical Institute Medical Research Fellow. **Author contributions:** M.M.K. planned animal breedings and qPCR experiments and performed monosynaptic rabies tracing, electrophysiology experiments, calcium imaging recordings, immunohistochemistry, and data analysis. M.M.K., K.L.B., and B.B.B. optimized vagal cuff protocol and initial data analysis. K.L.B. performed all vagal cuff recordings, immunohistochemistry, and data analysis. M.E.K. manufactured monosynaptic rabies strains, culture organoids, rabies infection of enteroendocrine cells in organoids, organoid-nodose monosynaptic tracing, and data analysis. M.M.M. performed all animal breeding, mouse colony management, genotyping, and quality control. X.S. advised with biomedical implants, including abdominal window, as well as data analysis. M.M.K. and D.V.B. planned experiments and composed figures. D.V.B. conceptualized, acquired funding for, and supervised the project, as well as wrote the final manuscript. **Competing interests:** Some of the findings in this manuscript have been used to file a provisional patent application. No other competing interests are declared. **Data and materials availability:** All data are available in the manuscript or the supplementary materials.

SUPPLEMENTARY MATERIALS

www.sciencemag.org/content/361/6408/eaat5236/suppl/DC1
Materials and Methods
Figs. S1 to 20
Table S1
References (*30*–*37*)
Movies S1 and S2
Data S1

12 March 2018; accepted 2 August 2018
10.1126/science.aat5236

A gut-brain neural circuit for nutrient sensory transduction

Melanie Maya Kaelberer, Kelly L. Buchanan, Marguerita E. Klein, Bradley B. Barth, Marcia M. Montoya, Xiling Shen and Diego V. Bohórquez

Science **361** (6408), eaat5236.
DOI: 10.1126/science.aat5236

Dissecting the gut-brain axis

It is generally believed that cells in the gut transduce sensory information through the paracrine action of hormones. Kaelberer *et al.* found that, in addition to the well-described classical paracrine transduction, enteroendocrine cells also form fast, excitatory synapses with vagal afferents (see the Perspective by Hoffman and Lumpkin). This more direct circuit for gut-brain signaling uses glutamate as a neurotransmitter. Thus, sensory cues that stimulate the gut could potentially be manipulated to influence specific brain functions and behavior, including those linked to food choices.

Science, this issue p. eaat5236; see also p. 1203